



HHS Public Access

Author manuscript

Nanomedicine. Author manuscript; available in PMC 2015 November 01.

Published in final edited form as:

Nanomedicine. 2014 November ; 10(8): 1777–1785. doi:10.1016/j.nano.2014.06.010.

Atomic force microscopy reveals age-dependent changes in nanomechanical properties of the extracellular matrix of native human menisci: implications for joint degeneration and osteoarthritis

Jeanie Kwok, MS^{a,b,d}, Shawn Grogan, PhD^d, Brian Meckes, CPhil^c, Fernando Arce, PhD^{a,c}, Ratnesh Lal, PhD^{a,b,c}, and Darryl D'Lima, MD, PhD^d

^aDepartment of Mechanical and Aerospace Engineering, University of California, San Diego, 9500 Gilman Drive, La Jolla, CA 92093

^bMaterials Science and Engineering Program, University of California, San Diego, 9500 Gilman Drive, La Jolla, CA 92093

^cDepartment of Bioengineering, University of California, San Diego, 9500 Gilman Drive, La Jolla, CA 92093

^dShiley Center for Orthopaedic Research and Education at Scripps Clinic, 11025 North Torrey Pines Road, Suite 200, La Jolla, CA 92037

Abstract

With aging, the menisci become more susceptible to degeneration due to sustained mechanical stress accompanied by age-related changes in the extracellular matrix (ECM). However, the mechanistic relationship between age-related meniscal degeneration and osteoarthritis (OA) development is not yet fully understood. We have examined the nanomechanical properties of the ECM of normal, aged, and degenerated human menisci using atomic force microscopy (AFM). Nanomechanical profiles revealed a unique differential qualitative nanomechanical profile of healthy young tissue: prominent unimodal peaks in the elastic moduli distribution among three different regions (outer, middle, and inner). Healthy aged tissue showed similar differential elasticity for the three regions but with both unimodal and bimodal distributions that included higher elastic moduli. In contrast, degenerated OA tissue showed the broadest distribution without prominent peaks indicative of substantially increased heterogeneity in the ECM mechanical properties. AFM analysis reveals distinct regional nanomechanical profiles that underlie aging dependent tissue degeneration and OA.

© 2014 Elsevier Inc. All rights reserved.

Corresponding authors and addresses: Ratnesh Lal, University of California, San Diego, 9500 Gilman Drive, MC 0412, La Jolla, CA 92093, Phone: (858) 822-0384, rlal@eng.ucsd.edu. Darryl D'Lima, Shiley Center for Orthopaedic Research and Education at Scripps Clinic, 11025 North Torrey Pines Road, Suite 200, La Jolla, CA 92037, Phone: (858) 332-0166, DLima.Darryl@scrippshealth.org.

The authors report no conflicts of interest.

Publisher's Disclaimer: This is a PDF file of an unedited manuscript that has been accepted for publication. As a service to our customers we are providing this early version of the manuscript. The manuscript will undergo copyediting, typesetting, and review of the resulting proof before it is published in its final citable form. Please note that during the production process errors may be discovered which could affect the content, and all legal disclaimers that apply to the journal pertain.

Keywords

Atomic force microscopy; Meniscus; Nanomechanics; Osteoarthritis

Background

Aging is the leading risk factor for osteoarthritis (OA), a whole joint degenerative disease that affects all articulating tissues, including articular cartilage and menisci in the knee. The menisci play a crucial role in joint loading by providing mechanical stability, smooth articulation, shock absorption, load bearing and transmission in the knee.¹⁻⁷ Damage or degeneration due to aging of the menisci leads to unfavorable changes in joint loading that significantly affect overall joint health by precipitating the onset of OA development. The role of meniscal injuries and surgical removal of the meniscus on the development of post-traumatic OA is well established.⁸⁻¹⁰ However, the mechanistic relationship between age-related meniscal degeneration and OA development is not yet fully understood.

The menisci are two crescent shaped tissue structures wedged between the articulating surfaces of the femoral condyle and tibial plateau. During normal joint loading, the femoral condyle bears down on the menisci concentrating the highest compressive loads in the inner tapered end of the tissue. The forces are transmitted to the outer periphery due to its geometry, which causes the tissue to expand circumferentially. The extrusion is resisted by the anterior and posterior attachments, creating circumferential tensile hoop stresses that distribute the compressive load. This anisotropic biomechanical response is supported by a regionally heterogeneous network of collagenous extracellular matrix (ECM) that varies in microvasculature, microstructure, and biocomposition.^{11, 12} The inner region is composed primarily of randomly aligned collagen type II fibrils embedded within an abundance of proteoglycan molecules that help resist high compressive loads.^{13, 14} The outer region is more fibrous consisting of both collagen types I and II that form mostly circumferentially aligned fibrils to uphold tensile strength and carry out anisotropic load transmission.^{13, 14}

Age-related changes are accompanied by molecular and structural changes in the ECM that lead to matrix degeneration.¹⁵⁻¹⁷ This degenerative process is characterized by an imbalance between anabolic and catabolic processes as cells reduce production of important growth factors and increase production of matrix degrading enzymes and inflammatory cytokines.^{18, 19} These age-related biochemical changes have been identified by histological analyses which demonstrate increased Safranin-O staining, reduced cellularity, and loss of collagen fiber orientation.²⁰ While the biochemical changes have been investigated by histological and immunohistochemical analyses, age-related changes in biomechanical properties have not been documented at the microstructural level in human menisci. Our hypothesis is that aging alters the biomechanical properties of meniscal ECM thus changing the tissue response during joint loading thereby leading to OA development.

To define the earliest age-related biomechanical changes of the ECM, a high resolution force scanning technique is required to measure mechanical properties at the nano-to-microscale, the native length scale of the cells and associated matrix. Recent studies have examined tissue mechanical properties at the nano-to-microscale utilizing atomic force

microscopy (AFM).²¹ Cartilaginous tissues, including articular cartilage and porcine menisci, have been evaluated by AFM demonstrating depth-dependent and regional variations in nanomechanical properties.^{22, 23} However, the nanomechanical properties of human meniscal tissue, especially in its native and non-fixed condition, have not been reported. Characterizing these nanomechanical properties and identifying key changes with aging, degeneration, and OA will provide important insights into the pathogenesis of joint degeneration and OA, and may lead to novel therapeutic developments for the prevention and treatment of OA. For tissue engineering of menisci, nanomechanical characterization is critical for optimal design of materials and scaffolds. In addition, understanding the correlation between biochemical and biomechanical changes may lead to novel targets for pharmacological modulation of meniscal tissue degeneration.

In this study, we have examined nanomechanical properties of the ECM of normal, aged, and osteoarthritic human menisci using AFM. Human meniscal tissue samples were collected from donors of various ages and OA grades to represent meniscus physiology of aging and OA development. Regional ECM nanomechanical properties of individual specimens were measured by AFM-based elastic mapping and correlated with histological Safranin-O staining to identify matrix degeneration.²⁴ Our results show distinct regional differences in the nanomechanical properties of menisci that correlate well with the aging as well as with the severity of OA.

Methods

Tissue selection and processing

This study was approved by the Institutional Review Board at Scripps Health. Human knee joints were collected from tissue banks or from patients undergoing total knee arthroplasty. Subjects were selected by age and OA grade scored by macroscopic assessment of articular cartilage.²⁵ Briefly, OA grade 0 describes normal (intact smooth surface) articular cartilage, grade 1 thru 3 describes surface irregularities of slight to moderate reductions, and grade 4 describes severe disruption or loss of tissue.²⁵

In this study, 8 individual specimens were selected to represent normal meniscus physiology and pathophysiology, grouped by age and OA grade (age range 20–90 years; OA grade 0–4). Tissue donors were separated into three groups: specimens from individuals younger than 45 and of OA grade 0 were classified as young normal menisci; specimens from individuals older than 50 with OA grade 1 to 2 were classified as aging normal; and severely degenerated human menisci obtained from OA knee joints (OA grade 4) removed from patients greater than 50 years of age and undergoing total knee arthroplasty were classified as aging OA.

Menisci were dissected from the knee joints and triangular shaped cross-sections in the sagittal plane were harvested from the central portion of the medial menisci (Fig 1). The samples were embedded into O.C.T. Tissue Tek (Sakura Finetek, Torrance, CA) and stored at –80 °C for cryopreservation. The O.C.T. embedded samples were then cut using a cryostat microtome into 10 µm thick sections onto glass slides to be processed for histology

and AFM measurements. Same or adjacent tissue sections were evaluated by AFM using histology to locate regions of interest.

10 μm thick cryosections were thawed and stained with Safranin-O/Fast Green (Sigma-Aldrich, St. Louis, MO) for semi-quantitative evaluation of proteoglycan content associated with matrix degeneration. Each tissue section was examined for Safranin-O staining intensity.

Atomic force microscopy

Prior to AFM, the tissue sections were thawed, having undergone only one freeze-thaw cycle to minimize the effects of freezing on the tissue structure. Tissue sections were rinsed with PBS to remove O.C.T. Tissue Tek and replenished with fresh PBS (Cellgro, Manassas, VA) to allow the tissue to swell at room temperature. All AFM measurements were carried out using a diBioScope SZ AFM (Bruker Corporation, Santa Barbara, CA) mounted on an Olympus IX71 inverted microscope used to visually position the AFM cantilever with respect to the sample. Colloidal AFM cantilevers (silicon nitride rectangular cantilever tip with a 5 μm diameter borosilicate glass sphere attached; NovaScan, Ames, IA) were used. The nominal spring constant k of the cantilever was 4.5 N/m and the exact value was determined by the thermal tuning method. The deflection sensitivity was determined by indenting on a glass substrate in fluid. Force-volume (FV) maps were generated from $20 \times 20 \mu\text{m}^2$ to $50 \times 50 \mu\text{m}^2$ areas of the tissue samples. Each FV map recorded 32×32 pixels (1024 force-displacement curves per map). Each individual force curve constitutes 512 data points. The maximum applied loading force was $\sim 200\text{nN}$, which resulted in indentation depths of $\sim 1 \mu\text{m}$ ($\sim 10\%$ of the section thickness) at a tip velocity of $\sim 15 \mu\text{m/s}$. Force retraction curves were analyzed using Hertzian contact mechanics to determine the elastic modulus. The Poisson's ratio was assumed to be 0.04.

Statistical analyses

All elastic measurements were summarized in histogram plots to obtain the distribution of values. The bin width was set at 20 kPa while the frequency count was normalized to the total number of measurements per region. A multi-peak Gaussian curve fit was applied to the distribution wherein peaks were located using the peak analysis in OriginPro 7.0 (Northampton, MA). All data are presented as a mean \pm standard deviation. The statistical significance of differences between stiffness values from different regions (outer, middle, and inner) and conditions (normal, aged, and OA) were assessed by Kruskal-Wallis nonparametric test followed by a Wilcoxon test with a Bonferroni correction for age group comparisons in R 3.1.0.

Results

Nanomechanical properties of ECM of menisci in normal joints

Histological analyses of meniscus specimens from three young normal individuals (20, 31, and 41 years of age) showed healthy, normal well-organized ECM with minimal Safranin-O staining, and intact articular surfaces (Fig 2). Individual histograms of regional ECM elastic moduli characterized the nanomechanical profile for healthy, young normal menisci with

distinct unimodal peaks in distribution (Figure 2). In general, the outer and middle regions were characterized by a sharp dominant peak at 130 to 150 kPa and the inner region at 70 to 90 kPa. Mean elastic moduli also varied with regions: the outer region with its characteristic fibrous content measured the highest in elastic moduli with a mean value of 205.6 ± 8.9 , with the middle region showing the next highest with a mean value of 188.0 ± 21.9 kPa (Table 1). The inner region displayed the lowest elastic moduli with a mean value of 176.7 ± 28.0 kPa. Each region was statistically different ($P < 0.05$).

Nanomechanical properties of ECM of menisci in aged joints

Meniscus specimens representative of normal aging (55 and 56 years of age; OA grade 1 and 2, respectively) exhibited intact articular surfaces, organized matrix, and mild matrix degeneration reflected in the slight to moderate increase in Safranin-O staining compared to healthy normal ECM. Histograms showed a nanomechanical profile that was similar to young, normal menisci with distinct peaks that were comparable in magnitude. However, the elastic moduli of normal aged specimens were more widely distributed, as reflected in the larger standard deviation, and included stiffer values. In addition, the wider distribution contained bimodal peaks varying from 110 to 400 kPa (Figure 3).

In the sample of 55 years of age (OA grade 1), the outer region exhibited a wider (bimodal) distribution compared to the middle and inner regions (unimodal), which still displayed region-defined nanomechanical properties. However, in the sample of 56 years of age (OA grade 2), region-defined nanomechanical properties became less distinct in nanomechanical properties among the outer (303.0 ± 28.3 kPa), middle (282.4 ± 30.2 kPa), and inner regions (274.0 ± 8.7 kPa).

Nanomechanical properties of ECM of menisci in osteoarthritic joints

All OA specimens were harvested from patients with undergoing total knee arthroplasty. Macroscopic and histopathological analyses of the articular cartilage were categorized as OA grade 4, while histological assessment of menisci showed severe matrix degeneration as identified by intense Safranin-O staining throughout the sample. OA menisci specimens exhibited a characteristic wide spread distribution of nanomechanical properties with no dominant peak. The wide distribution of elastic moduli demonstrates stiffer mean values in the outer (364.3 ± 72.2 kPa), middle (401.9 ± 39.2 kPa), and inner regions (365.9 ± 106.5) (Figure 4). The large standard deviations indicate increased nanomechanical heterogeneity that correlated with increased Safranin-O staining intensity in matching sections. Notably, each individual OA sample displayed a unique nanomechanical profile of each region. The regions were not statistically significantly different ($P > 0.05$).

Correlation of nanomechanical properties of ECM to histological analyses

The respective nanomechanical profiles were correlated with the histopathological findings in normal, aged, and degenerated OA human meniscal tissue. The correlation of local AFM measurements with matching Safranin-O stained sections corroborated that the ECM regions with strong staining intensity exhibit stiffer values. This pattern was more pronounced in OA samples, as the strong Safranin-O staining in the outer regions was associated with broader and stiffer values (~ 300 to 350 kPa) compared to the middle and inner regions

(Figure 4). Figure 5 summarizes the characteristic nanomechanical profile of normal, normal aged, and OA human menisci.

Discussion

Meniscal degeneration due to aging and OA remains poorly understood. In accordance with conventional knowledge (mostly from experimental animal models), studies of macroscopic and histopathological changes of the menisci demonstrate a strong association between age-related meniscal degeneration and OA.^{16, 17, 26–28} This is supported by clinical findings of a high incidence of OA in middle to advanced ages that occurs concomitantly with meniscal lesions.^{29–31} Studies on animal tissues provide for a convenient assessment of anatomical, biochemical, and biomechanical properties of the menisci,^{16, 17, 23, 32–35} but are biased due to interspecies variations raised by significant differences in size, shape, matrix architecture and biochemical content.³⁶

This study is the first to document age-related biomechanical changes in native human menisci during tissue degeneration and OA development. An experimental profile of human meniscal tissue samples from individuals of various ages and degenerated/diseased conditions were examined to characterize age-related changes. Histological analyses of the samples collectively showed a clear representation of aged-related changes, as evidenced by a marked increase in Safranin-O staining with age. We used AFM-based elasticity mapping of tissue samples to characterize regional nanomechanical properties in normal, aged, and degenerated OA menisci. Overall, these results showed a similar trend in regional nanomechanical properties in healthy young menisci compared to properties previously reported on porcine menisci, although human tissue proved to be less stiff than porcine.²³ Like porcine menisci, the outer region of human menisci is stiffer due to its characteristic collagen fiber I fibrous content, while the inner region is more compliant in line with its rich proteoglycan content. This regional definition of nanomechanical properties is important to the overall health and function of the meniscus, as the results show that the regional properties become less defined with aging and disease (Figure 5). Indeed, regional differences in nanomechanical properties of OA samples proved to be statistically insignificant ($P > 0.05$). Loss of mechanical integrity is likely to compromise the biomechanical function of the tissue, disrupting the region-defined anisotropic biomechanical response of the tissue for efficient load bearing and transmission. These findings suggest that changes in regional nanomechanical properties in the ECM may emerge from earlier biochemical changes that occur during aging and take part in the initiation and progression of OA.

The most striking finding in this study is that normal, aged, and osteoarthritic human meniscal tissue exhibited qualitatively unique nanomechanical profiles. Young, healthy tissues exhibited a unimodal distribution in elastic moduli with each region displaying distinctly sharp peaks: outer (130 to 150 kPa), middle (130 – 150 kPa), and inner (70 – 90 kPa). Normal aged tissue also exhibited similar unimodal peaks but with a wider distribution (often bimodal) biased towards stiffer values. In general, the bimodal distributions encompassed a narrow first peak and broader second peak, suggesting regions of increased stiffness associated with degeneration. This bimodality was more obvious in some samples

compared to others reflective of the severity of degeneration. Within the nanomechanical profiles, age-related changes associated with matrix degeneration were recognized by two features: (i) increased nanomechanical heterogeneity in line with increased Safranin-O staining and (ii) development of matrix stiffening with wider distributions.

Additionally, nanomechanical evaluations of degenerated OA samples were each individually unique in regional properties and distribution profiles. These results demonstrated incremental heterogeneity in nanomechanical properties with aging and OA development. Indeed, OA manifests as a heterogeneous disease with varying clinical features and biochemical characteristics among patients.^{37, 38}

In general, with increasing age there is stiffening of tissue, which is likely to increase the compressive stiffness of the overall tissue. Eventually, this leads to compromised tensile strength leading to biomechanical failure. Matrix stiffening is most likely due to age-related molecular changes in the ECM, such as abnormal deposition and cross-linking of ECM molecules.^{39–41} These changes are known to alter matrix mechanics which can lead to abnormal cell behavior.^{42–46} Meniscal cells are highly responsive to mechanical stimuli during joint loading.^{47–50} It is possible these changes in the ECM may cause or exacerbate OA-associated phenotypic changes in cells. However, the precise relationship between matrix mechanics and OA development remains to be established.

In summary, we have characterized regional nanomechanical properties of human meniscal tissue, especially ECM changes that occur during aging and OA. Further studies should investigate the correlation between biomechanical properties and biochemical characteristics that reflect meniscal tissue degeneration and OA. Understanding these age-related degenerative changes will provide insight for the development of effective therapeutic strategies to prevent and treat OA.

Acknowledgments

This work was supported by NIH Grants P01 AG007996 (D.D.) and R01DA025296 (R.L.). We greatly appreciate the technical assistance by Merissa Olmer, Lilo Creighton, and Nick Glembotski.

References

1. Ahmed A, Burke D. In-Vitro of Measurement of Static Pressure Distribution in Synovial Joints—Part I: Tibial Surface of the Knee. *Journal of biomechanical engineering*. 1983; 105:216–25. [PubMed: 6688842]
2. Mow VC, Ratcliffe A. Structure and function of articular cartilage and meniscus. *Basic orthopaedic biomechanics*. 1997; 2:113–77.
3. Proctor C, Schmidt M, Whipple R, Kelly M, Mow V. Material properties of the normal medial bovine meniscus. *Journal of Orthopaedic Research*. 1989; 7:771–82. [PubMed: 2677284]
4. Radin EL, de Lamotte F, Maquet P. Role of the menisci in the distribution of stress in the knee. *Clinical orthopaedics and related research*. 1984; 185:290–4. [PubMed: 6546709]
5. Seedhom B, Hargreaves D. Transmission of the Load in the Knee Joint with Special Reference to the Role of the Menisci Part II: Experimental Results, Discussion and Conclusions. *Engineering in Medicine*. 1979; 8:220–8.
6. Shoemaker S, Markolf K. The role of the meniscus in the anterior-posterior stability of the loaded anterior cruciate-deficient knee. Effects of partial versus total excision. *The Journal of Bone & Joint Surgery*. 1986; 68:71–9. [PubMed: 3753605]

7. Shrive N, O'connor J, Goodfellow J. Load-bearing in the knee joint. *Clinical orthopaedics and related research*. 1978; 131:279–87. [PubMed: 657636]
8. Fairbank T. Knee joint changes after meniscectomy. *Journal of Bone & Joint Surgery, British Volume*. 1948; 30:664–70.
9. Krause W, Pope M, Johnson R, Wilder D. Mechanical changes in the knee after meniscectomy. *The Journal of bone and joint surgery American volume*. 1976; 58:599–604. [PubMed: 946970]
10. Lohmander LS, Englund PM, Dahl LL, Roos EM. The long-term consequence of anterior cruciate ligament and meniscus injuries osteoarthritis. *The American journal of sports medicine*. 2007; 35:1756–69. [PubMed: 17761605]
11. Arnoczky SP, Warren RF. Microvasculature of the human meniscus. *The American journal of sports medicine*. 1982; 10:90–5. [PubMed: 7081532]
12. Day B, Mackenzie W, Shim SS, Leung G. The vascular and nerve supply of the human meniscus. *Arthroscopy: The Journal of Arthroscopic & Related Surgery*. 1985; 1:58–62.
13. Aspden R, Yarker Y, Hukins D. Collagen orientations in the meniscus of the knee joint. *Journal of anatomy*. 1985; 140:371. [PubMed: 4066476]
14. MCDEVITT CA, WEBBER RJ. The ultrastructure and biochemistry of meniscal cartilage. *Clinical orthopaedics and related research*. 1990; 252:8–18. [PubMed: 2406077]
15. Adams ME, Billingham ME, Muir H. The glycosaminoglycans in menisci in experimental and natural osteoarthritis. *Arthritis & Rheumatism*. 1983; 26:69–76. [PubMed: 6401994]
16. Hellio Le Graverand M-P, Vignon E, Otterness I, Hart D. Early changes in lapine menisci during osteoarthritis development: Part I: cellular and matrix alterations. *Osteoarthritis and Cartilage*. 2001; 9:56–64. [PubMed: 11178948]
17. Hellio Le Graverand M-P, Vignon E, Otterness I, Hart D. Early changes in lapine menisci during osteoarthritis development Part II: Molecular alterations. *Osteoarthritis and Cartilage*. 2001; 9:65–72. [PubMed: 11178949]
18. Herwig J, Egner E, Buddecke E. Chemical changes of human knee joint menisci in various stages of degeneration. *Annals of the rheumatic diseases*. 1984; 43:635–40. [PubMed: 6548109]
19. Ishihara G, Kojima T, Saito Y, Ishiguro N. Roles of metalloproteinase-3 and aggrecanase 1 and 2 in aggrecan cleavage during human meniscus degeneration. *Orthopedic reviews*. 2009:1.
20. Pauli C, Grogan S, Patil S, et al. Macroscopic and histopathologic analysis of human knee menisci in aging and osteoarthritis. *Osteoarthritis and Cartilage*. 2011; 19:1132–41. [PubMed: 21683797]
21. Binnig G, Quate CF, Gerber C. Atomic force microscope. *Physical review letters*. 1986; 56:930. [PubMed: 10033323]
22. McLeod MA, Wilusz RE, Guilak F. Depth-dependent anisotropy of the micromechanical properties of the extracellular and pericellular matrices of articular cartilage evaluated via atomic force microscopy. *Journal of biomechanics*. 2013; 46:586–92. [PubMed: 23062866]
23. Sanchez-Adams J, Wilusz RE, Guilak F. Atomic force microscopy reveals regional variations in the micromechanical properties of the pericellular and extracellular matrices of the meniscus. *Journal of Orthopaedic Research*. 2013; 31:1218–25. [PubMed: 23568545]
24. Rosenberg L. Chemical basis for the histological use of safranin O in the study of articular cartilage. *The Journal of Bone & Joint Surgery*. 1971; 53:69–82. [PubMed: 4250366]
25. Pauli C, Whiteside R, Heras F, et al. Comparison of cartilage histopathology assessment systems on human knee joints at all stages of osteoarthritis development. *Osteoarthritis and Cartilage*. 2012; 20:476–85. [PubMed: 22353747]
26. Burman MS, Sutro CJ. A study of the degenerative changes of the menisci of the knee joint, and the clinical significance thereof. *The Journal of Bone & Joint Surgery*. 1933; 15:835–61.
27. Englund M. The role of the meniscus in osteoarthritis genesis. *Medical Clinics of North America*. 2009; 93:37–43. [PubMed: 19059020]
28. Loeser RF. Age-related changes in the musculoskeletal system and the development of osteoarthritis. *Clinics in geriatric medicine*. 2010; 26:371. [PubMed: 20699160]
29. Bhattacharyya T, Gale D, Dewire P, et al. The Clinical Importance of Meniscal Tears Demonstrated by Magnetic Resonance Imaging in Osteoarthritis of the Knee*. *The Journal of Bone & Joint Surgery*. 2003; 85:4–9. [PubMed: 12533565]

30. Englund M, Guermazi A, Gale D, et al. Incidental meniscal findings on knee MRI in middle-aged and elderly persons. *New England Journal of Medicine*. 2008; 359:1108–15. [PubMed: 18784100]
31. Makris EA, Hadidi P, Athanasiou KA. The knee meniscus: structure–function, pathophysiology, current repair techniques, and prospects for regeneration. *Biomaterials*. 2011; 32:7411–31. [PubMed: 21764438]
32. Arnoczky SP, Warren RF. The microvasculature of the meniscus and its response to injury An experimental study in the dog. *The American journal of sports medicine*. 1983; 11:131–41. [PubMed: 6688156]
33. Cox JS, Nye CE, Schaefer WW, Woodstein IJ. The degenerative effects of partial and total resection of the medial meniscus in dogs' knees. *Clinical orthopaedics and related research*. 1975; 109:178–83. [PubMed: 1173359]
34. McDevitt C, MuIR H. Biochemical changes in the cartilage of the knee in experimental and natural osteoarthritis in the dog. *Journal of Bone & Joint Surgery, British Volume*. 1976; 58:94–101.
35. Nakano T, Dodd CM, Scott PG. Glycosaminoglycans and proteoglycans from different zones of the porcine knee meniscus. *Journal of orthopaedic research*. 1997; 15:213–20. [PubMed: 9167623]
36. Joshi MD, Suh JK, Marui T, Woo SLY. Interspecies variation of compressive biomechanical properties of the meniscus. *Journal of biomedical materials research*. 1995; 29:823–8. [PubMed: 7593020]
37. Driban JB, Sitler MR, Barbe MF, Balasubramanian E. Is osteoarthritis a heterogeneous disease that can be stratified into subsets? *Clinical rheumatology*. 2010; 29:123–31. [PubMed: 19924499]
38. Felson DT, Lawrence RC, Dieppe PA, et al. Osteoarthritis: new insights. Part 1: the disease and its risk factors. *Annals of internal medicine*. 2000; 133:635–46. [PubMed: 11033593]
39. Wang X, Shen X, Li X, Mauli Agrawal C. Age-related changes in the collagen network and toughness of bone. *Bone*. 2002; 31:1–7. [PubMed: 12110404]
40. Verzijl N, DEGROOT J, OLDEHINKEL E, et al. Age-related accumulation of Maillard reaction products in human articular cartilage collagen. *Biochem J*. 2000; 350:381–7. [PubMed: 10947951]
41. Verzijl N, DeGroot J, Zaken CB, et al. Crosslinking by advanced glycation end products increases the stiffness of the collagen network in human articular cartilage: a possible mechanism through which age is a risk factor for osteoarthritis. *Arthritis & Rheumatism*. 2002; 46:114–23. [PubMed: 11822407]
42. Ingber DE. Tensegrity: the architectural basis of cellular mechanotransduction. *Annual review of physiology*. 1997; 59:575–99.
43. Ingber DE. Mechanobiology and diseases of mechanotransduction. *Annals of medicine*. 2003; 35:564–77. [PubMed: 14708967]
44. Wang N, Butler JP, Ingber DE. Mechanotransduction across the cell surface and through the cytoskeleton. *Science*. 1993; 260:1124–7. [PubMed: 7684161]
45. Wang N, Tytell JD, Ingber DE. Mechanotransduction at a distance: mechanically coupling the extracellular matrix with the nucleus. *Nature reviews Molecular cell biology*. 2009; 10:75–82.
46. Discher DE, Janmey P, Wang Y-I. Tissue cells feel and respond to the stiffness of their substrate. *Science*. 2005; 310:1139–43. [PubMed: 16293750]
47. Fink C, Fermor B, Weinberg J, Pisetsky D, Misukonis M, Guilak F. The effect of dynamic mechanical compression on nitric oxide production in the meniscus. *Osteoarthritis and Cartilage*. 2001; 9:481–7. [PubMed: 11467897]
48. Fermor B, Jeffcoat D, Hennerbichler A, Pisetsky DS, Weinberg JB, Guilak F. The effects of cyclic mechanical strain and tumor necrosis factor alpha on the response of cells of the meniscus. *Osteoarthritis and cartilage*. 2004; 12:956–62. [PubMed: 15564062]
49. Upton ML, Chen J, Guilak F, Setton LA. Differential effects of static and dynamic compression on meniscal cell gene expression. *Journal of orthopaedic research*. 2003; 21:963–9. [PubMed: 14554206]
50. Upton ML, Guilak F, Laursen TA, Setton LA. Finite element modeling predictions of region-specific cell-matrix mechanics in the meniscus. *Biomechanics and modeling in mechanobiology*. 2006; 5:140–9. [PubMed: 16520958]

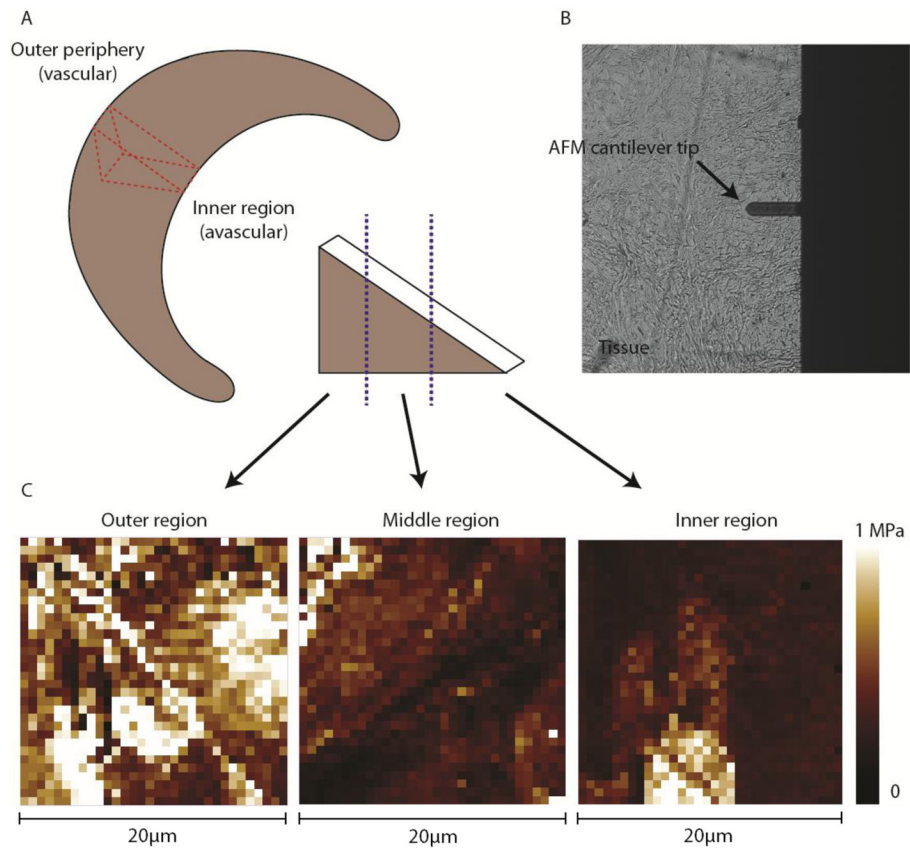


Figure 1. AFM schematics for force mapping of human meniscal tissue. (A) Central portion of medial meniscus was sectioned in the sagittal direction (red). The sagittal tissue portion was cut by a cryostat microtome at a thickness of 10 μm . The regions were defined by the purple line as the outer one-third, middle, and inner one-third of the tissue. (B) AFM cantilever tip with a glass microsphere attached (5 μm in diameter) was used to probe the tissue sample surface of the ECM. (C) Representative force maps (scan size of 20 μm \times 20 μm) of outer, middle, and inner regions were generated from which the elastic moduli was extracted and plotted in histogram distributions.

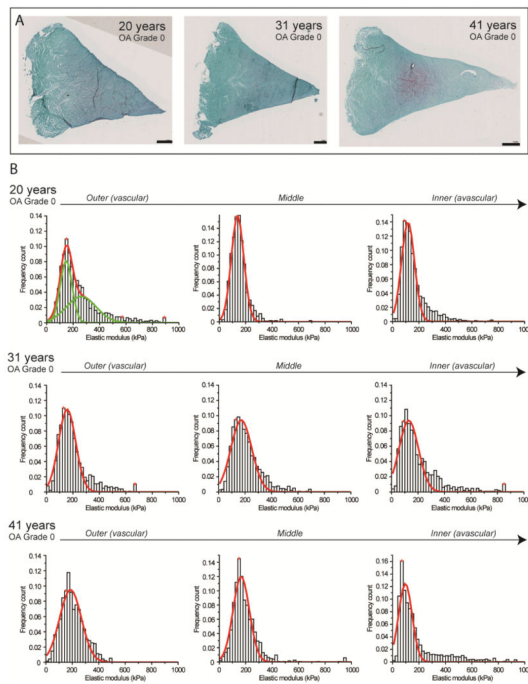


Figure 2. Nanomechanical properties of ECM of healthy normal human meniscal tissue with OA grade 0–1. (A) Histological overview of the samples shows minimal Safranin-O staining (in purple) indicating young, normal meniscal tissue. Scale bar = 1 mm. (B) Corresponding stiffness distributions with a multi-peak Gaussian curve fit (in red and green) reveals sharp distinct peaks within each region, representing regional differences across the tissue: outer and middle (peak values from 130 to 150 kPa) and inner region (peak values from 70 to 90 kPa).

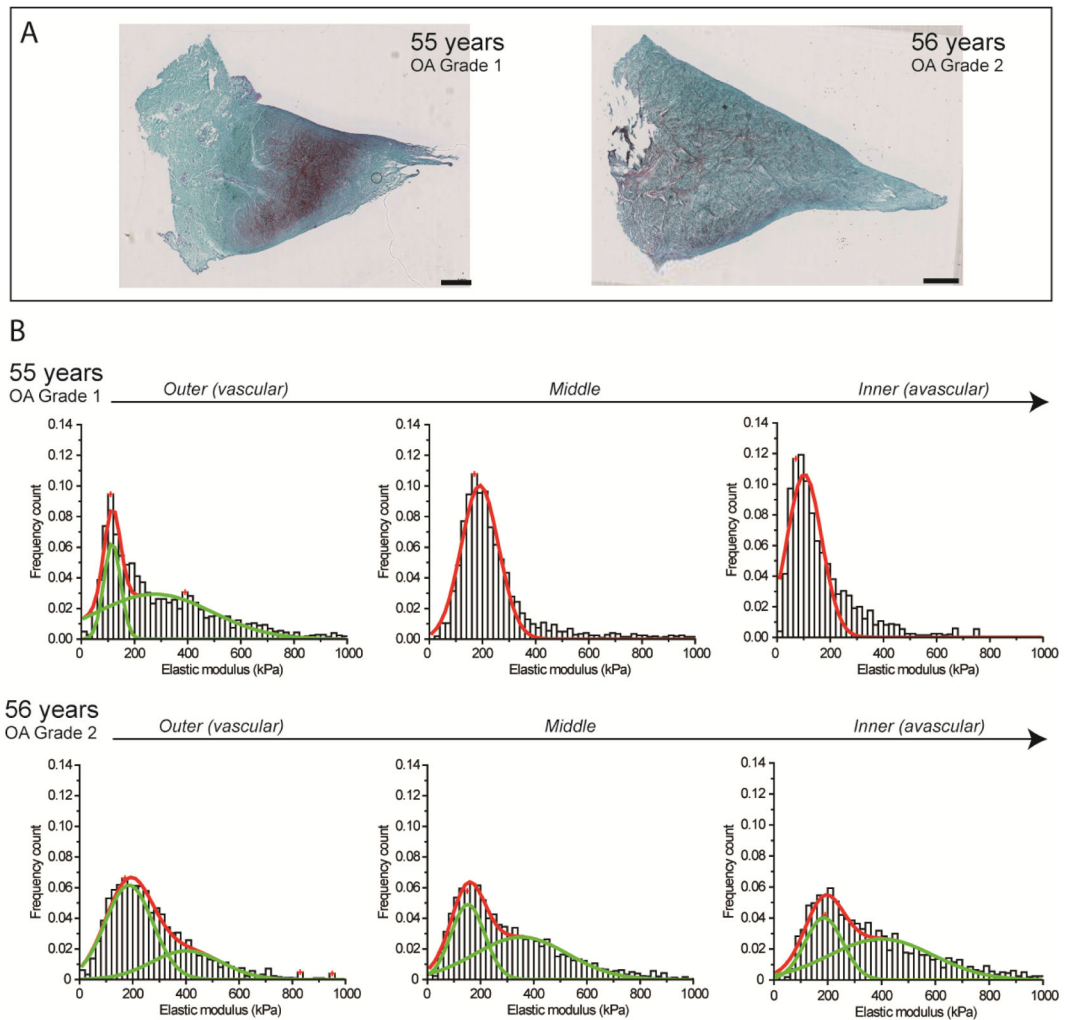


Figure 3.

Nanomechanical properties of ECM of aged human meniscal tissue with OA grade 1–2. (A) Histological analyses of normal aging samples shows slight to moderate Safranin-O staining (in purple) typical of normal tissue degeneration due to aging. Scale bar = 1 mm. (B) Stiffness distribution with multi-peak Gaussian fit curves (in red) revealed both unimodal and bimodal (in green) distributions with regional variations but with a broader distribution that shifts towards stiffer values with increasing age.

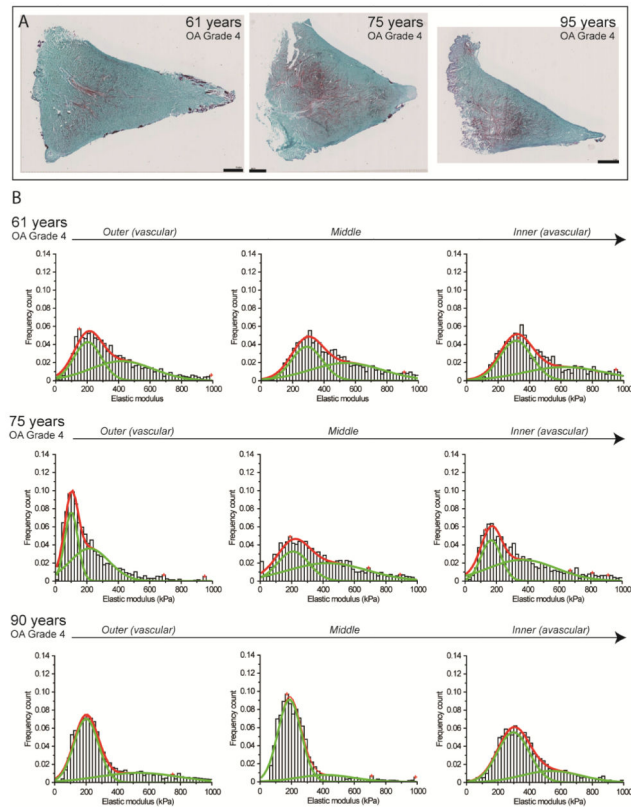


Figure 4. Nanomechanical properties of ECM of degenerated human meniscal tissue removed from patients with severe OA undergoing total knee arthroplasty. (A) Histopathology of all three OA samples show a more intense Safranin-O staining (in purple) associated with severe matrix degenerative changes in the ECM. Scale bar = 1 mm. (B) Corresponding elastic moduli distributions with multi-peak Gaussian curve fits (in red) demonstrate a significant increase in stiffness with broadened bimodal distributions (in green) and increased nanomechanical heterogeneity across regions (from outer to inner, left to right).

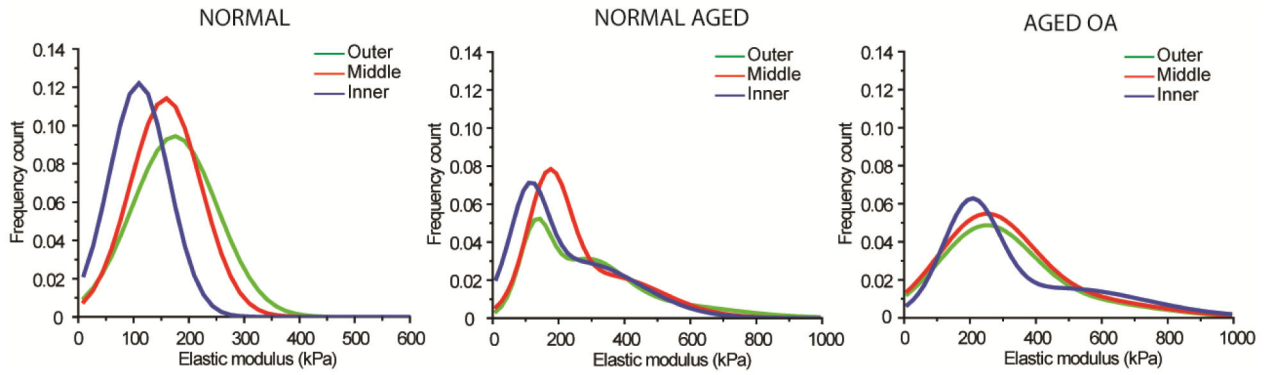


Figure 5.

Nanomechanical profiles for normal, aged, and degenerated OA human menisci revealed unique qualitative representation of aging and degenerated/diseased conditions. Healthy normal meniscal tissue present narrow distinct peaks of the three regions while normal aged and degenerated OA samples display a broadened bimodal distribution indicative of increased mechanical heterogeneity across all regions.

Mean elastic moduli determined from individual donor samples belonging in three groups: normal, aged, and degenerated OA human menisci.

Table 1

Age populations (years)	Tissue Condition	OA diagnosis (cartilage)	Elastic modulus (kPa)		
			<i>Outer</i>	<i>Middle</i>	<i>Inner</i>
20, 31, 41	Normal	0-1	205.6 ± 8.9	188.0 ± 21.9	176.7 ± 28.0
55, 56	Normal Aged	1-2	303.0 ± 28.3	282.4 ± 30.2	274.0 ± 8.7
61, 75, 90	Aged OA	4 (TKA)	364.3 ± 72.2	401.9 ± 39.2	365.9 ± 106.5

* OA (osteoarthritis)

[†]TKA (total knee arthroplasty)